

Inductively Coupled Plasma Reactive Ion Etching of AlGaAsSb and InGaAsSb for Quaternary
Antimonide MIM Thermophotovoltaics

M.N. Palmisano
Bechtel Bettis, Inc.

G.M. Peake, R.J. Shul, C.I. Ashby, J.G. Cederberg, M.J. Hafich, R.M. Biefeld
Sandia National Laboratory

N00024-98-C-4064

NOTICE

This report was prepared as an account of work sponsored by the United States Government. Neither the United States, nor the United States Department of Energy, nor the United States Navy, nor any of their employees, nor any of their contractors, subcontractors, or their employees, makes any warranty, express or implied, or assumes any legal liability or responsibility for the accuracy, completeness or usefulness of any information, apparatus, product or process disclosed, or represents that its use would not infringe privately owned rights.

BETTIS ATOMIC POWER LABORATORY

WEST MIFFLIN, PENNSYLVANIA 15122-0079

Operated for the U.S. Department of Energy
by Bechtel Bettis, Inc.

Inductively Coupled Plasma Reactive Ion Etching of AlGaAsSb and InGaAsSb for Quaternary Antimonide MIM Thermophotovoltaics

Greg M. Peake, Randy J. Shul, Carol I. Ashby, Jeff G. Cederberg, Mike J. Hafich and

Robert M. Biefeld

Sandia National Laboratories

Marc N. Palmisano

Bechtel Bettis Atomic Laboratory

Abstract

In this letter we report on the inductively coupled plasma reactive ion etching (ICP-RIE) of InGaAsSb and AlGaAsSb for the fabrication of quaternary monolithic interconnected module (MIM) thermophotovoltaic (TPV) devices. A rapid dry etch process is described that produces smooth surfaces using BCl_3 for AlGaAsSb and InGaAsSb capped with GaSb. Uncapped InGaAsSb was etched by adding an H_2 plasma preclean to reduce surface oxides. InGaAsSb etch rate was studied as a function of accelerating voltage, RF power, temperature and pressure. The etch conditions found for InGaAsSb were used for AlGaAsSb etching to determine the effectiveness for isolation of the MIM cells.

I. Introduction

Research in thermophotovoltaic (TPV) devices has been renewed by recent progress in the growth of quaternary antimonide materials with a bandgap near 0.5 eV.^{1, 2, 3, 4} This bandgap is appropriate for blackbody photon emitters with $T \sim 1100$ K.⁵ InGaAsSb TPV devices promise performance superior to the ternary devices due, in part, to the ability of the quaternaries to grow lattice matched to a GaSb substrate. Because of the lack of an insulating substrate, AlGaAsSb cell isolation diodes are currently used in the MIM structure⁶ and we have demonstrated a series wiring technique to electrically connect adjacent isolated cells.⁷

Current fabrication techniques for TPV devices have relied on wet chemistry for etching and there is preliminary evidence that the wet chemical etches are less damaging to cell isolation and TPV diodes. However, wet etching of III-Sb materials with high Al mole fraction yields slow etch rates and rough surfaces.⁸ Dry etch schemes are more attractive for device manufacturing due to the anisotropic profiles that can be produced along with increased etch uniformity and reproducibility. Additionally, in-situ reflectance can be used to monitor the etch and provide precise control over the etch depth. Improved reverse current behavior of GaSb/InGaAsSb diodes treated with H_2+N_2 plasma at $450^\circ C$ ⁹ suggests that post etch treatments could be used mitigate some of the dry etch damage.

Dry etching of InSb and GaSb has been reported using ECR^{10, 11, 12}, CAIBE¹³ and RIE¹⁴ discharges. Vawter et al.¹⁵ have reported the reactive ion beam etching of InAsSb-based strained-layer superlattices. However, there have been few reports of acceptable etches for the quaternary antimonide materials. Piotrowska et al.¹⁶ found CCl_4/H_2 to give good etch rates for the quaternaries but sidewall damage and poor morphology are a concern with this technique. Quaternary antimonide multiple-quantum-well structures were etched using ECR plasmas¹⁷ at relatively slow etch rates (45 nm/min) which

indicated low-damage by photoluminescence measurements. Zhang et. al¹⁸ have reported the etching of AlGaAsSb using inductively coupled plasma reactive ion etching (ICP-RIE) and achieved etch rates near 500 nm/min. with smooth surfaces and anisotropic profiles.

For MIM TPV structures it is critical to determine the conditions for low-damage etching to reduce leakage current through the CIDs to the substrate. ICP-RIE etches are thought to be more economical for scaling and power requirements than other low damage etches and have a more mature automatic tuning technology. In our current configuration, the etch gases are introduced through an annulus at the top of the chamber. The ICP power is used to apply rf to an inductive coil surrounding a dielectric vessel that controls the plasma density by inducing a strong alternating magnetic field. Independent control of the ion bombardment is achieved by superimposing a DC self-bias on the sample. Lower pressures can lead to enhanced anisotropy as gas phase collisions are minimized. Temperature can have a significant effect on the chemical/physical nature of the etch as higher temperatures can increase etch product volatility and surface reactivity. Temperature control has many beneficial effects including improved anisotropy and morphology.

II. ICP-RIE of InGaAsSb and AlGaAsSb with cap layers

All of the structures used in the experiment were grown in an Emcore D-125 or modified D-75 high speed rotating disk reactor using triethylgallium, ethyldimethylamine, triethylantimony, and arsine for the AlGaAsSb layers; and using triethylgallium, trimethylantimony, tertiarybutylarsine and trimethylindium for the InGaAsSb layers. The samples were patterned with AZ4330 photoresist and mounted using a temperature conductive paste on an anodized Al carrier that is clamped to the cathode and cooled with He gas in the etch chamber. Etching was performed in a loadlocked PlasmaTherm SLR 770 ICP reactor with the ICP source at 2 MHz and a DC self-bias of 13.56 MHz on the sample. In-situ reflectance monitors and a Tencor alpha-step were used to determine etch rates. RMS roughness was measured with a Nanoscope Atomic Force Microscope.

Table 1. summarizes the results of our attempts at etching InGaAsSb and defines the etch conditions for samples A-M. The samples were nominally 1 micron of InGaAsSb with a 100 nm GaSb cap layer. The baseline condition for the InGaAsSb etch experiments was sample A with 500 W ICP power, 250 V DC bias, 2.5 mTorr pressure and a carrier temperature of 10°C. For the experiments with the capped material we used 40 sccm of BCl_3 for the etch gas.

	DC Bias (V)	ICP Power (W)	Pressure (mTorr)	Temperature (°C)	rms rough (nm)
A	250	500	2.5	10	0.397
B	150	500	2.5	10	0.46
C	350	500	2.5	10	2.354
D	50	500	2.5	10	10.433
E	250	400	2.5	10	1.774
F	250	300	2.5	10	1.315
G	250	200	2.5	10	0.758
H	250	500	2.5	-10	0.567
I	250	500	2.5	25	0.581
J	250	500	2.5	35	1.619
K	250	500	10	10	2.845
L	250	500	7.5	10	1.846
M	250	500	5	10	0.608

Table 1. ICP RIE Etch Matrix for InGaAsSb. Varied parameters are highlighted for clarity.

As can be seen in Figure 1, the etch rate increases sublinearly as more ions are accelerated to the sample. Initially, as ion energy increases, the etch rate will increase due to improved sputter desorption efficiency of the etch products from the surface. In addition, higher ion energy improves the ability to break surface bonds which essentially increases the reactivity of the surface and reaction kinetics of the etch gases. However, as the ion energy continues to increase, it is possible to reach a state where the ions sputter the reactants from the surface before they can react.

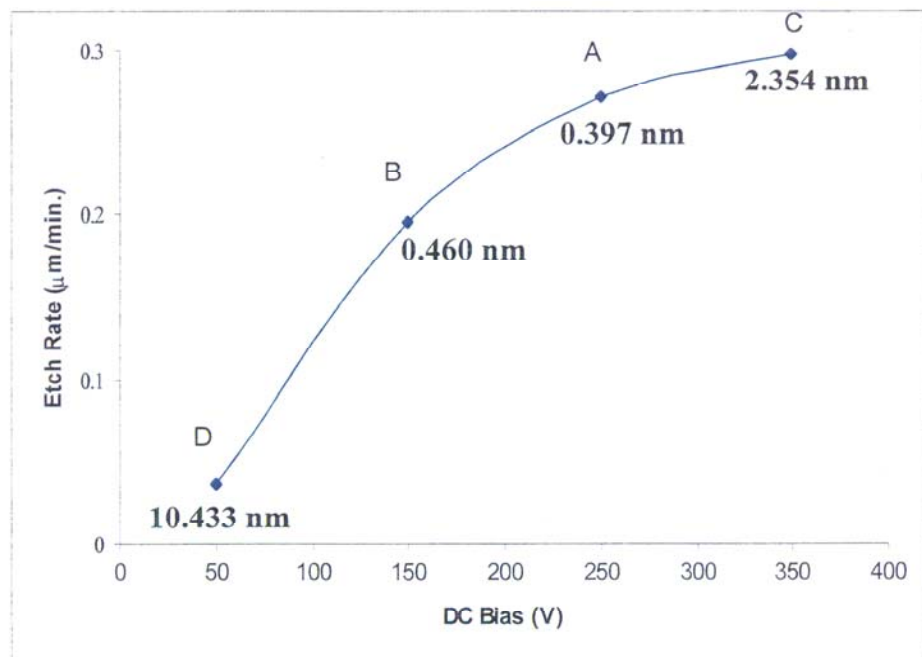


Figure 1. InGaAsSb etch rate as a function of DC Bias accelerating voltage.

The numbers alongside the data points are the RMS surface roughness taken from atomic force microscopy (AFM) measurements. Figure 2. shows an AFM of the baseline condition (sample A).

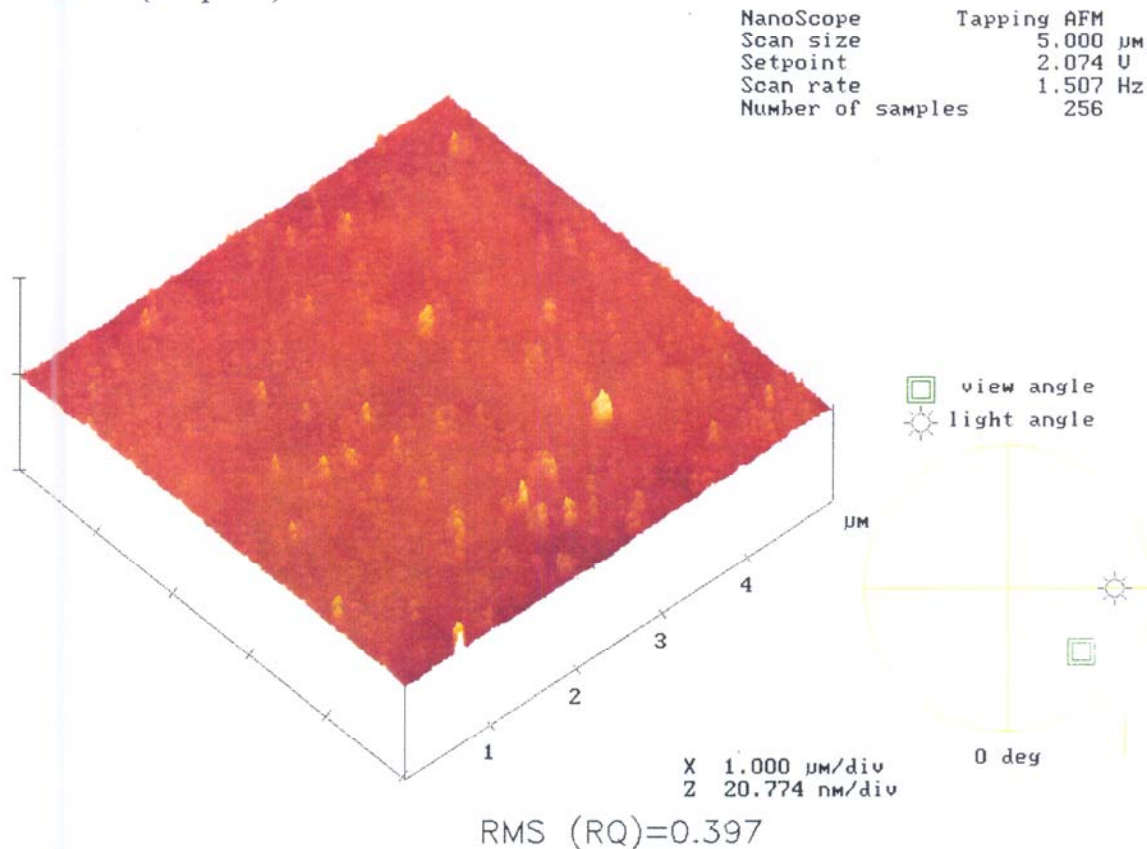


Figure 2. AFM of sample A etched with the baseline conditions.

For an accelerating voltage of 250 V, a reduction in surface roughness is measured. We propose that this is due to the proper ratio of neutral and ion-energy flux at the plasma-surface interaction layer. Further chemical studies need to be undertaken to verify this ratio for chemical damage mechanisms, however physical damage is minimized at the baseline condition. As shown in Figure 3, the sample with the lowest DC Bias exhibits surface roughening that may be due to preferential etching or micromasking effects.

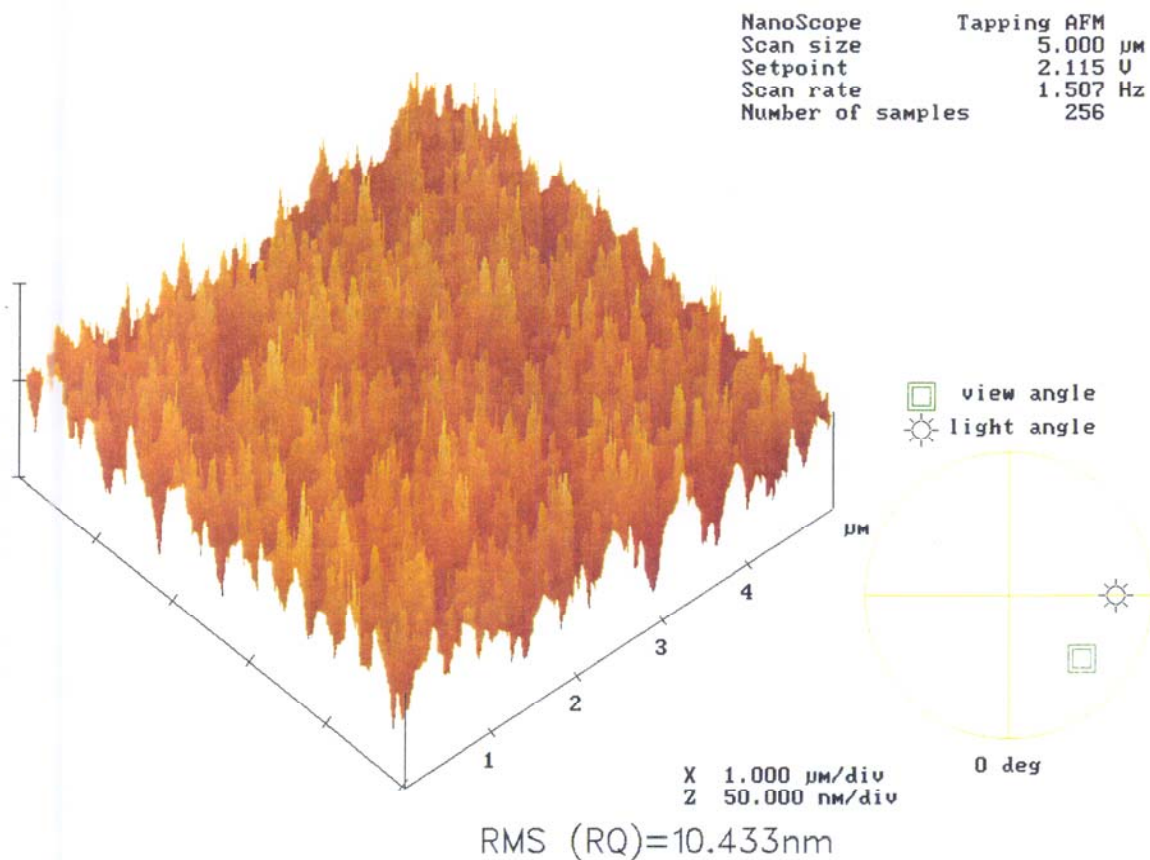


Figure 3. Surface roughening of sample D with low DC Bias.

As the ICP power is increased, ion and neutral density (plasma density) increases. This can often lead to higher etch rates, however, at high densities the surface may become saturated with reactants and in some cases passivated to the point that the etch rate decreases. Additionally, an increase in the plasma density reduces the mean free path and the ion energy may decrease due to a higher collision frequency. Figure 4. shows a relatively linear etch rate as a function of ICP power indicative of controlled physical sputtering using ion-bombardment. Again the baseline conditions exhibit the least physical damage along with the highest etch rate. Higher etch rates would lead to a lack of etch depth control so it was not practical to include bounding data points for this parametric variation.

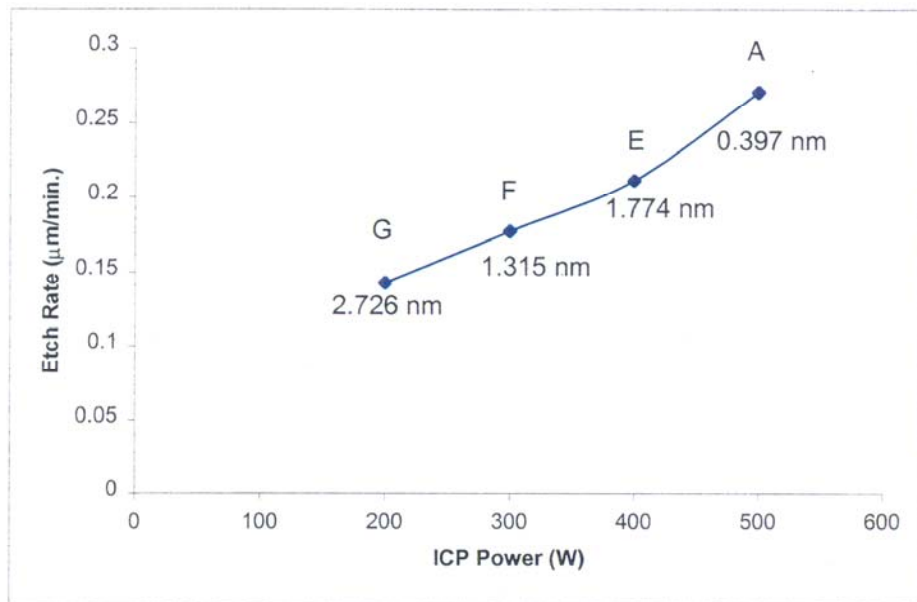


Figure 4. InGaAsSb etch rate as a function of ICP power.

Figure 5. illustrates a low variability of etch rate with temperature which is consistent with a physical sputtering mechanism. However, as the temperature is raised the film roughens possibly due to the different volatility of etch products or higher reactivity of the surface.

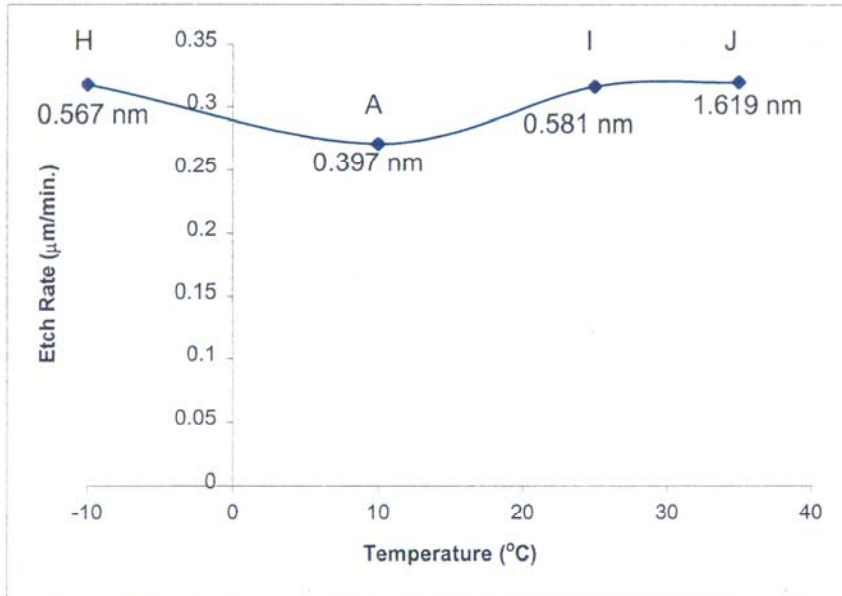


Figure 5. InGaAsSb etch rate as a function of substrate temperature.

Finally, the etch rate was measured as a function of pressure as shown in Figure 6. Pressures lower than 2 mTorr were not investigated due to the difficulty of striking a plasma at reduced pressures.

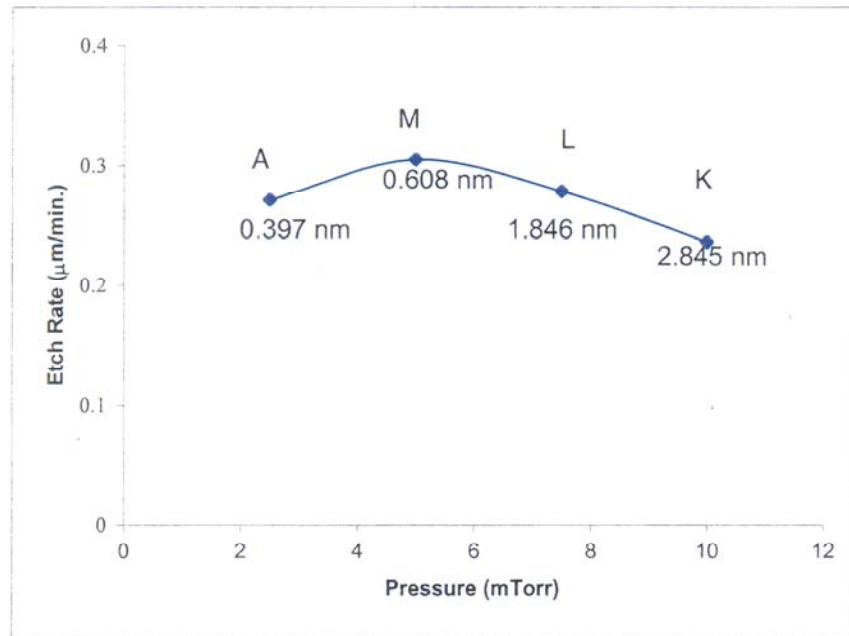


Figure 6. InGaAsSb etch rate as a function of pressure.

The initial increase in etch rate from 2 to 4 mTorr suggests a reactant limited etch regime for the baseline etch as a higher pressure yields more reactive Cl species. As the pressure is increased above 4 mTorr, increased collision frequency lowers the kinetic energy of the ions indicative of a sputtering desorption limited etch mechanism.

Since the AlGaAsSb cell isolation diode and InGaAsSb thermophotovoltaic diode must be etched through for isolation of the MIM device, it is prudent to use the same conditions for both materials. We have found that the baseline conditions for the InGaAsSb can be used for AlGaAsSb. Using these conditions we obtain etch rates of 3000 Å/min. and RMS surface roughness of 2.3 nm which is greater than the InGaAsSb roughness but acceptable for our purposes. A detailed parametric study of AlGaAsSb etched with BCl_3/Ar plasma ICP-RIE in this chamber can be found in reference 18.

IV. ICP-RIE of InGaAsSb with thinner cap layers

The ICP-RIE of InGaAsSb with a thin or no cap layer proved to be more difficult as a rapidly forming oxide inhibited the etch and produced poor surface morphology. Figure 7. is an SEM of the result of using the baseline etch procedure with no surface preparation to remove the native oxides.

Adding a high-mass atom to the plasma often sputters the oxide from the surface and reduces the etch resistance of the surface caused by oxides and impurities. Figure 8 shows our attempts adding argon to the plasma. The conditions for this etch were the same as the baseline etch with 40 sccm of BCl_3 and 5 sccm of Ar.

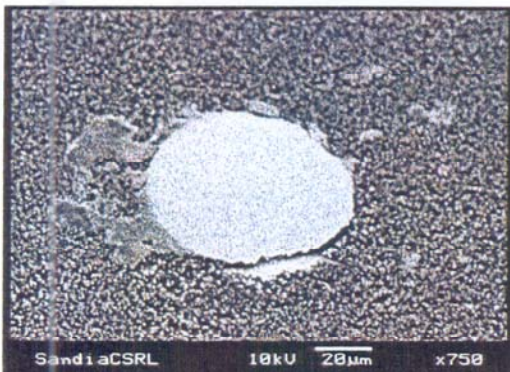


Figure 7. BCl_3 with no oxide removal

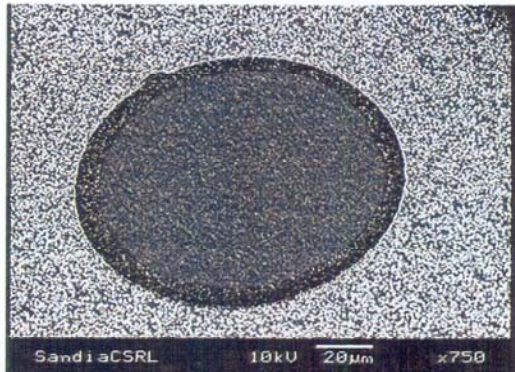


Figure 8. BCl_3 with Ar sputtering

This allowed some etching, however the rates were extremely low and the surface morphology was poor with RMS roughness >10 nm. Figure 9 is an attempt to remove surface oxides ex-situ with $1\text{HCl}:1\text{H}_2\text{O}$ for 3 minutes prior to the BCl_3 /Ar etch.

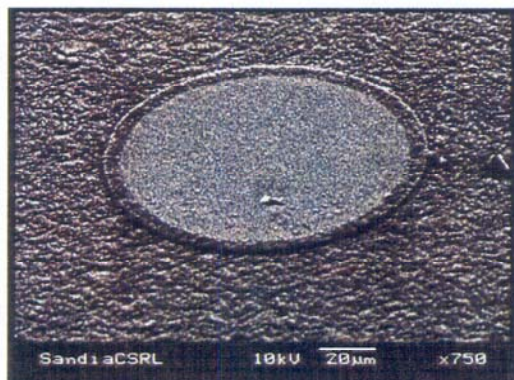


Figure 9. BCl_3+Ar etch with ex-situ oxide removal

Again this resulted in poor morphology and very low etch rates. Addition of 5 sccm Cl_2 instead of Ar had similar results. Figure 10 shows this same feature treated with an in-situ hydrogen plasma clean prior to a BCl_3 ICP-RIE etch along with a close-up of another smaller feature. Our pre-clean treatment consisted of a 30 sccm H_2 flow, 5 sccm Ar flow, pressure at 15 mTorr, -10°C cathode temperature with 500 W ICP power and 40 V DC Bias. The reflectance was monitored in-situ until a threshold value was reached indicating a clean etch surface. This preclean was immediately followed by the baseline 40 sccm etch with similar etch rates as seen for the capped structures. We propose that there is a rapidly forming oxide on the InGaAsSb that inhibits the etch as has been reported for GaSb.¹⁹ By removing the oxide, the etch is allowed to proceed. Interestingly, we have found this problem only on the InGaAsSb samples and the AlGaAsSb samples have never required the preclean treatment.

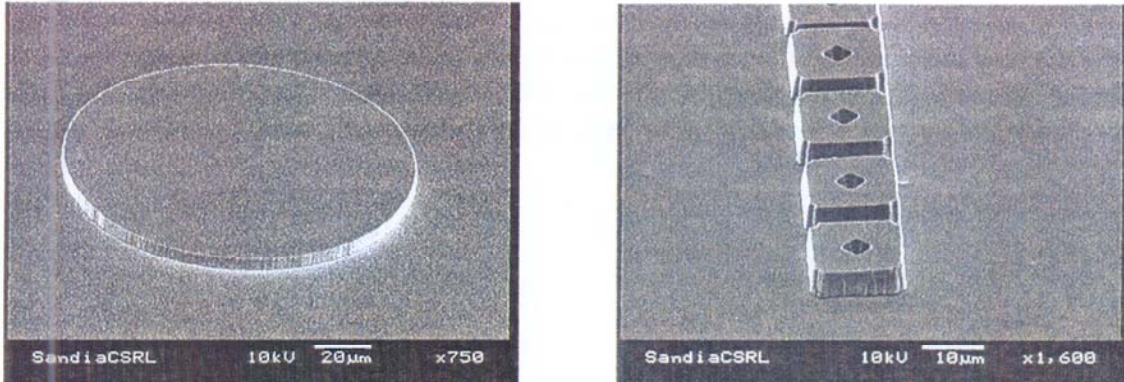


Figure 10. BCl_3 etch with in-situ preclean treatment and smaller feature with higher magnification.

The RMS roughness was measured at 0.410 nm by AFM in the etch field and this is similar to the best results using the baseline etch developed in the previous section.

Conclusions

We have demonstrated a rapid etch technology that can be used for InGaAsSb and AlGaAsSb for the fabrication of MIM TPV devices. Etch rates of 2700 Å/min with RMS roughness of 0.397 nm and 3000 Å/min. with RMS roughness of 2.33 nm were demonstrated for InGaAsSb and AlGaAsSb respectively. At these conditions physical sputtering dominates the etch characteristics. InGaAsSb samples with thin or no cap layer required the addition of an H_2 preclean treatment to remove surface oxides before the etch was effective.

Acknowledgments

The authors are grateful to M. White and L. Griego for assistance in the preparation and characterization of these materials. This work was supported by the US DOE under Contract No. DE-AC04-94AL85000. Sandia is a multiprogram laboratory operated by Sandia Corporation, a Lockheed Martin Company, for the United States Department of Energy.

¹ M.N. Palmasiano, R.M. Biefeld, J.G. Cederberg, M.J. Hafich, and G.M. Peake, 5th Conference on Thermophotovoltaic Generation of Electricity, Como, Italy (2001).

² C. A. Wang, H.K. Choi, S. L. Ransom, G. W. Charache, L. R. Danielson, and E. M. DePoy, *Appl. Phys. Lett.* **75**, 1305 (1999).

³ G.W. Charache, P.F. Baldasaro, L.R. Danielson, D.M. DePo, M.J. Freeman, C.A. Wang, H.K. Choi, D.A. Garbuzov, R.U. Martinelli, V. Khalfin, S. Saroop, J.M. Borrego and R.J. Gutmann, *J. Appl. Phys.* **85**, pp. 2247-2252 (1999).

⁴ V.B. Khalfin, D.Z. Garbuzov, H. Lee, G.C. Taylor, N. Morris, R.U. Martinelli and J.C. Connolly, 4th NREL Conf. Thermophotovoltaic Generation of Electricity, Devner, Co (1998).

⁵ T. Coutts, C. Allman and J. BennerEds., 3rd NREL Conf. Thermophotovoltaic Generation of Electricity, AIP Conf. Proc. 401 (1997).

⁶ G.M. Peake, J.G. Cederberg, M.J. Hafich and R.M. Biefeld, MIM TPV conference, Pleasant Hills, Pa (2000).

⁷ G.M. Peake, J.G. Cederberg, M.J. Hafich and R.M. Biefeld, to be published in *Journal of the Electrochemical Society*.

⁸ G.C. Desalvo, R. Kaspi and C.A. Bozado, *J. Electrochem. Soc.* **141**, 3526 (1994).

⁹ A.Y. Polyakov, A.G. Milnes, X Li, A.A. Balmashnov and N.B. Smirnov, *Sol. State Electron.* **38** (10), 1743 (1995).

¹⁰ S.J. Pearton, F. Ren and C.R. Abernathy, *Appl. Phys. Lett.* **64**, 1673 (1994).

¹¹ L.R. Mileham, J.W. Lee, E.S. Lambers and S.J. Pearton, *Semicond. Sci. Technol.* **12**, 338 (1997).

¹² J.W. Lee, J. Hong, E.S. Lambers, C.R. Abernathy, S.J. Pearton, W.S. Hobson and F. Ren, *J. Electron. Mater.* **26**, 429 (1997).

¹³ G. Nagy, R.U. Ahmad, M. Levy, R.M. Osgood, M.J. Manfra and G.W. Turner, *Appl. Phys. Lett.*, 72 (11) 1350 (1998).

¹⁴ S.S. Ou, *J. Vac. Sc. Technol. B*, **14** (5), 3226 (1996).

¹⁵ G.A. Vawter and J.R. Wendt, *Appl. Phys. Lett.* **58** (3), 21 (1991).

¹⁶ A. Piotrowska, E. Kamińska, T.T. Piotrowski, M. Guziewicz, K. Głońska, E. Papis, *j. Wrbel and L. Perchucki, Vacuum* **56**, 57 (2000).

¹⁷ R.U. Ahmad, G. Nagy, R.M. Osgood, G.W. Turner, M.J. Mangra and J. W. Chludzinski, *Appl. Phys. Lett.* **77** (7) 1008 (2000).

¹⁸ L. Zhang, L.F. Lester, R.J. Shul, C.G. Willison and R.P. Leavitt, *J. Vac. Sci. Technol. B* **17** (3), 965 (1999).

¹⁹ M. Kodomam, *Adv. Mat. Opt. Electron.*, **4**, 319 (1994).